HHS Public Access

Author manuscript

Biochim Biophys Acta Mol Cell Biol Lipids. Author manuscript; available in PMC 2024 June 06.

Published in final edited form as:

Biochim Biophys Acta Mol Cell Biol Lipids. 2023 October ; 1868(10): 159366. doi:10.1016/j.bbalip.2023.159366.

Endoplasmic reticulum stress and mitochondrial dysfunction during aging: Role of sphingolipids

Qun Chen[a], **Anna Kovilakath**[b], **Jeremy Allegood**[b], **Jeremy Thompson**[a], **Ying Hu**[a], **L. Ashley Cowart**[b,d], **Edward J. Lesnefsky**[a,b,c,d,*]

[a]Department of Medicine (Division of Cardiology), Virginia Commonwealth University, Richmond, VA 23298, United States of America

[b]Department of Biochemistry and Molecular Biology, Virginia Commonwealth University, Richmond, VA 23298, United States of America

[c]Department of Physiology and Biophysics, Virginia Commonwealth University, Richmond, VA 23298, United States of America

[d]Richmond Department of Veterans Affairs Medical Center, Richmond, VA 23249, United States of America

Abstract

The endoplasmic reticulum (ER) plays a key role in the regulation of protein folding, lipid synthesis, calcium homeostasis, and serves as a primary site of sphingolipid biosynthesis. ER stress (ER dysfunction) participates in the development of mitochondrial dysfunction during aging. Mitochondria are in close contact with the ER through shared mitochondria associated membranes (MAM). Alteration of sphingolipids contributes to mitochondria-driven cell injury. Cardiolipin is a phospholipid that is critical to maintain enzyme activity in the electron transport chain. The aim of the current study was to characterize the changes in sphingolipids and cardiolipin in ER, MAM, and mitochondria during the progression of aging in young (3 mo.), middle (18 mo.), and aged (24 mo.) C57Bl/6 mouse hearts. ER stress increased in hearts from 18 mo. mice and mice exhibited mitochondrial dysfunction by 24 mo. Hearts were pooled to isolate ER, MAM, and subsarcolemmal mitochondria (SSM). LC-MS/MS quantification of lipid content showed that aging increased ceramide content in ER and MAM. In addition, the contents of sphingomyelin and monohexosylceramides are also increased in the ER from aged mice. Aging increased the total cardiolipin content in the ER. Aging did not alter the total cardiolipin content in mitochondria or MAM yet altered the composition of cardiolipin with aging in line with increased

*Corresponding author at: Cardiology Section, Medical Service 111(J) Richmond VA Medical Center, 1201 Broad Rock Boulevard, Richmond, VA 23249, United States of America. edward.lesnefsky@va.gov, edward.lesnefsky1@vcuhealth.org (E.J. Lesnefsky).

CRediT authorship contribution statement

Qun Chen: Conceptualization, Data curation, Funding acquisition, Investigation, Project administration, Supervision, Validation, Writing – original draft, Writing – review & editing. **Anna Kovilakath:** Data curation, Formal analysis, Investigation, Methodology, Resources, Validation, Writing – original draft, Writing – review & editing. **Jeremy Allegood:** Conceptualization, Data curation, Formal analysis, Investigation, Methodology, Resources, Supervision, Validation. **Jeremy Thompson:** Data curation, Formal analysis, Investigation. **Ying Hu:** Data curation, Formal analysis, Investigation. **L. Ashley Cowart:** Conceptualization, Data curation, Formal analysis, Funding acquisition, Methodology, Project administration, Resources, Supervision, Writing – review & editing. **Edward J. Lesnefsky:** Conceptualization, Data curation, Funding acquisition, Methodology, Project administration, Resources, Supervision, Writing – original draft, Writing – review & editing.

oxidative stress compared to young mice. These results indicate that alteration of sphingolipids can contribute to the ER stress and mitochondrial dysfunction that occurs during aging.

Keywords

Aging; electron transport chain; Ceramide; Sphingomyelin; Monohexosylceramides

1. Introduction

Mitochondria are essential to maintain cardiovascular function, however, aging results in mitochondrial dysfunction that augments the severity of cardiovascular disease in the aged population [1]. Although progress has been made to understand the mechanisms of aging-induced mitochondrial defects, the exact factors that trigger mitochondrial dysfunction remain unclear. Mitochondria are connected to the endoplasmic reticulum (ER) through mitochondria associated membranes (MAM) [2,3]. The main function of the ER is to regulate protein folding, lipid synthesis, and calcium homeostasis [4]. The accumulation of unfolded/misfolded proteins within the ER causes ER dysfunction (ER stress) [5]. Although the initial ER stress response is an adaptive response to restore ER function, prolonged ER stress is detrimental to the cell and impairs mitochondrial function [5-7]. The ER stress response progressively increases during aging and contributes to the mitochondrial dysfunction that occurs [8,9].

Sphingolipids, which include ceramides, sphingosine, sphingosine-1-phosphate, sphingomyelins, and glycosphingolipids, are structural components of plasma and intracellular organelle membranes and contribute to many cellular functions under both normal and pathophysiological conditions [10,11]. Alterations in sphingolipids contribute to mitochondrial dysfunction in pathological conditions including aging, diabetes, cancer, and cardiovascular diseases, including by direct effects on mitochondria [12-14]. Sphingolipids are synthesized in the ER and can contribute to ER stress [15]. Thus, altered sphingolipid synthesis is a potential source of the mitochondrial dysfunction in aging, either via direct effects or the induction of ER stress.

Ceramides are synthesized by ceramide synthase enzymes (CerS) which are localized in the ER. Although ceramides can be generated catabolically by hydrolysis of sphingomyelin [16], the chronic elevation of ceramides, as observed with aging in the current study, usually arise from the de novo synthetic pathway. There are six isoforms of CerS enzymes, which differ in their preference for distinct acyl-CoA species for the N-acylation reaction. Ceramides are classified as medium (C12–14), long (C16–C18), very long (C20–C24), and ultralong (C26 and above) based on the N-linked fatty acid residue chain length. Distinct CerS and their ceramide species promote distinct biological outcomes in cardiomyocytes [17,18].

ER and mitochondria are connected through the MAM that functions in lipid transfer and calcium exchange. Sphingolipids including ceramides are present in the MAM [12]. Recent studies show that the MAM contributes a key role in regulating mitophagy, mitochondrial fusion and fission, as well as the activation of programmed cell death [19]. However,

the effect of aging on MAM composition, especially in the alteration of sphingolipid components, remains unclear.

Although the classic induction of ER stress occurs via misfolded proteins, it is increasingly recognized that perturbation of the membrane composition of the ER alters the protein folding environment and thereby can induce ER stress [20]. It is not surprising then, that ceramides, which are generated in the ER, induce ER stress [15]. Indeed, depending on the exact molecular species, ceramides increase both membrane thickness and rigidity, and thus can promote protein misfolding, aggregation, and inhibit protein trafficking. Ceramide species also act directly through ER stress effectors including IRE1 and ATF6 [15], the latter increased with aging in the heart [8,9]. However, there are also signaling pathways by which ceramides contribute to ER stress. [21]. On the other hand, emerging evidence also suggests the converse scenario that ER stress lies upstream of ceramide production, which may serve as a protective adaptation [22]. For example, thapsigargin treatment to induce ER stress increased ceramide content [23], and depletion of CerS2 enhanced ER stress [24]. Thus, whether ceramides induce or mitigate ER stress remains uncertain and may be context-dependent.

Cardiolipin is mainly present in the mitochondrial inner membrane [25] and is critical for energy generation by maintaining the optimal activity of the electron transport chain (ETC) [26,27]. Because oxidative stress is increased in aged heart mitochondria, cardiolipin, which is highly enriched in oxidative-sensitive linoleic acid (C18:2), is especially vulnerable to oxidative damage in aged heart mitochondria [28]. Thus, a decrease in cardiolipin content or an alteration in composition is a potential mechanism to induce ETC dysfunction during aging [29,30]. However, cardiolipin content and composition in both SSM and IFM were unchanged with aging in elderly 24 mo. Fischer 344 rats [31]. Thus, the role of cardiolipin alteration as a mechanism of age-induced ETC defects remains uncertain. In the current study, the content of cardiolipin was quantified in ER, MAM, and isolated mitochondria from 3, 18, and 24 mo. mice. Next, the content and composition of sphingolipids in ER, MAM, and isolated mitochondria from 3, 18, and 24 mo. mice were characterized. The results received from the current study will advance the understanding of the role of lipid alterations in the aging-induced defects that occur in cardiac mitochondria in the aging heart.

2. Methods

2.1. Animal model of aging and treatment

The Institutional Animal Care and Use Committees of Virginia Commonwealth University (VCU) and the Richmond Department of Veterans Affairs Medical Center approved the experimental protocols based on the Guide for the Care and Use of Laboratory Animals. Animal care and use complied with ARRIVE guidelines. C57BL/6 male mice [young (3 mo.), middle aged (18 mo.), and old aged (24 mo.)] were provided by National Institutes of Aging colony Charles River Laboratories (Wilmington, MA). Mice were anesthetized with pentobarbital (100 mg/kg, I.P.) and mouse hearts were collected under deep anesthesia. Five mouse hearts were pooled for ER, MAM, and mitochondrial isolation.

2.2. Isolation of SSM, MAM and ER from young and aged hearts

The pooled mouse hearts were minced and diluted with 10 mL MSM-EDTA buffer A [220 mM mannitol, 70 mM sucrose, 5 mM MOPS (3-(N-morpholino)propanesulfonic acid), and 1 mM EDTA]. The minced tissue was homogenized in MSM-EDTA buffer using the polytron homogenizer (Kinematica, Switzerland) at 14000 rpm for 2.5 s. The polytron homogenate was centrifuged at 500 ×*g* for 10 min at 4 °C. The supernatant was collected and centrifuged at 10,000 ×*g* for 30 min to generate a crude cytosol fraction (supernatant) and a crude fraction of SSM (pellet). The crude cytosol was centrifuged at 20,000 ×*g* for 10 min to remove residual broken mitochondria. The supernatant was centrifuged at 100,000 ×*g* for 60 min. The supernatant was purified cytosol, and the pellet was ER that was suspended in MSM-EDTA buffer for analysis. The crude SSM fraction was re-suspended in 200uL MSM-EDTA buffer and laid on 30 % percoll solution and centrifuged at 95,000 ×*g* for 30 min. The upper layer (crude MAM) was transferred to a clean centrifuge tube and diluted with 4 mL MSM-EDTA buffer. The lower layer (SSM) was also transferred to a clean centrifuge tube and diluted with 4 mL MSM-EDTA buffer. Both crude MAM and SSM were centrifuged at 10,000 ×*g* for 10 min. The supernatant from the MAM tube was transferred into a clean tube and centrifuged at 100,000 ×*g* for 60 min. to yield purified MAM. The SSM pellet was resuspended in 3 mL MSM-EDTA buffer and centrifuged at 10,000 ×*g* for 10 min. to yield purified SSM. The purified MAM and SSM were resuspended in MSM-EDTA buffer and aliquoted for later analysis [2].

2.3. Lipid extraction

All internal standards were purchased from Avanti Polar Lipids (Alabaster, AL), and the SPLASH LIPIDOMIX standard mix was used for untargeted analyses. This mixture included 15:0–18:1(d7) PC, 15:0–18:1(d7) PE, 15:0–18:1(d7) PS, 15:0–18:1(d7) PG, 15:0–18:1(d7) PI, 15:0–18:1(d7) PA, 18:1(d7) LPC, 18:1(d7) LPE, 18:1(d7) Cholesterol Ester, 18:1(d7) MAG, 15:0–18:1(d7) DAG, 15:0–18:1(d7)-15:0 TAG, 18:1(d9) SM, and Cholesterol (d7). For targeted sphingolipid analyses, internal standards were added to samples in 10 μL ethanol:methanol: water (7:2:1) as a cocktail of 250 pmol each. Standards for sphingoid bases and sphingoid base 1-phosphates were 17-carbon chain length analogs: C17-sphingosine, (2S,3R,4E)-2-aminoheptadec-4-ene-1,3-diol (d17:1-So); C17-sphinganine, (2*S*,3*R*)-2-aminoheptadecane-1,3-diol (d17:0-Sa); C17-sphingosine 1-phosphate, heptadecasphing-4-enine-1-phosphate (d17:1-So1P); and C17-sphinganine 1-phosphate, heptadecasphinganine-1-phosphate (d17:0-Sa1P). Standards for N-acyl sphingolipids were C12-fatty acid analogs: C12-Cer, N-(dodecanoyl)-sphing-4-enine (d18:1/C12:0); C12-Cer 1-phosphate, N-(dodecanoyl)-sphing-4-enine-1-phosphate (d18:1/C12:0-Cer1P); C12-sphingomyelin, N-(dodecanoyl)-sphing-4-enine-1-phosphocholine (d18:1/C12:0-SM); and C12-glucosylceramide, N-(dodecanoyl)-1-β-glucosyl-sphing-4-eine. For cardiolipin, a tetra C14:0 cardiolipin (Avanti Polar Lipids) was added as internal standard.

Samples were collected into 13 × 100 mm borosilicate tubes with a Teflon-lined cap (catalog #60827–453, VWR, West Chester, PA). Then 2 mL of CH_3OH and 1 mL of $CHCl_3$ were added along with the internal standards as above (10 μL). The contents were dispersed using an ultra sonicator at room temperature for 30 s. This single-phase mixture was incubated at 48 °C overnight. Debris was then pelleted in a centrifuge for 5 min. at 5000 ×*g*, and

the supernatant was transferred to a clean tube. The extract was reduced to dryness using a Speed Vac. The dried residue was reconstituted in 0.2 mL of the starting mobile phase solvent for untargeted analysis, sonicated for approximately 15 s., then centrifuged for 5 min. in a tabletop centrifuge (~5000 ×*g*) before transfer of the clear supernatant to the autoinjector vial for analysis.

2.4. Targeted analysis and phosphate assay

Lipid contents were measured in SSM, MAM, and ER. Sphingoid bases and complex sphingolipids including ceramides were separated by reverse phase LC using a Supelco 2.1 (i.d.) × 50 mm Ascentis Express C18 column (Sigma, St. Louis, MO) and a binary solvent system at a flow rate of 0.5 mL/min with a column oven set to 35 °C. Prior to injection of the sample, the column was equilibrated for 0.5 min with a solvent mixture of 95 % Mobile phase A1 ($CH_3OH/H_2O/HCOOH$, 58/41/1, v/v/v, with 5 mM ammonium formate) and 5 % Mobile phase B1 ($CH_3OH/HCOOH$, 99/1, v/v, with 5 mM ammonium formate), and after sample injection (typically 40 μL), the A1/B1 ratio was maintained at 95/5 for 2.25 min, followed by a linear gradient to 100 % B1 over 1.5 min, which was held at 100 % B1 for 5.5 min, followed by a 0.5 min gradient return to 95/5 A1/B1. The column was re-equilibrated with 95:5 A1/B1 for 0.5 min before the next run. For LC-MS/MS analyses, a Shimadzu Nexera LC-30 AD binary pump system coupled to a SIL-30 AC autoinjector and $DGU20A_{5R}$ degasser coupled to an AB Sciex 5500 quadrupole/linear ion trap (QTrap) (SCIEX Framingham, MA) operating in a triple quadrupole mode was used. Q1 and Q3 were set to pass molecularly distinctive precursor and product ions (or a scan across multiple *m/z* in Q1 or Q3), using N_2 to achieve collision induced dissociations in Q2 (which was offset from Q1 by 30–120 eV); the ion source temperature was set to 500 °C.

Cardiolipin was quantified on a Sciex 6500 QTrap mass spectrometer after separation by reverse phase LC using a Supelco 2.1 (i.d.) × 150 mm Ascentis Express C18 column (Sigma, St. Louis, MO) and a binary solvent system at a flow rate of 0.3 mL/min with a column temperature of 60 °C. Prior to injection of the sample, the column was equilibrated for 0.5 min with a solvent mixture of 30 % Mobile phase A (CH_3OH/H_2O, 50/50, v/v, with 2.5 mL triethylamine and 2.5 mL glacial acetic acid) and 70 % Mobile phase B (IPA/H_2O, 90/10, v/v, with 2.5 mL triethylamine and 2.5 mL glacial acetic acid), and after sample injection (typically 40 μL), the A/B ratio was maintained at 30/70 for 2.0 min, followed by a linear gradient to 100 % B over 7.0 min and held at 100 % B1 for 4.3 min, followed by a 0.6 min gradient return to 30/70 A/B. Each cardiolipin is quantified during each run by MRM analysis, and the structure is confirmed via a MS2 scan within the linear ion trap during the elution of each peak.

Data from targeted analyses were normalized by total phospholipid as determined by a standard published method [32]. In brief, a portion of lipid extract was dried down and dissolved in 0.6 mL ashing solution (0.8 N H_2SO_4, 1.4 % $HClO_4$ in H_2O). Samples were left overnight in a heating block at 160 °C. After this incubation, 0.9 mL water, 0.5 mL 0.9 % ammonium molybdate solution, and 0.2 mL 9 % ascorbic acid solution were added to the samples. Samples were incubated in a 45 °C water bath for ~30 min. Absorbance at 600 nm

was determined and phosphate amounts were extrapolated from a standard curve prepared from sodium phosphate solution.

2.5. Untargeted analysis

For LC-MS/MS analyses, a Thermo Scientific Q Exactive HF Hybrid Quadrupole-Orbitrap Mass Spectrometer was used. The lipids were separated by reverse phase LC using a Thermo Scientific Accucore Vanquish C18+ 2.1 (i.d.) × 150 mm column with 1.5 μm particles. The UHPLC used a binary solvent system at a flow rate of 0.26 mL/min with a column oven set to 55 °C. Prior to injection of the sample, the column was equilibrated for 2 min. With a solvent mixture of 99 % Moble phase A1 (CH_3CN/H_2O, 50/50, v/v, with 5 mM ammonium formate and 0.1 % formic acid) and 1 % Mobile phase B1 ($CH_3CHOHCH_3$/CH_3CN/H_2O, 88/10/2, v/v/v, with 5 mM ammonium formate and 0.1 % formic acid) and after sample injection (typically 10 μL), the A1/B1 ratio was maintained at 99/1 for 1.0 min, followed by a linear gradient to 35 % B1 over 2.0 min, then a linear gradient to 60 % B1 over 6 min, followed by a linear gradient to 100 % B1 over 11 min., which held at 100 % B1 for 5 min, followed by a 2.0 min gradient return to 99/1 A1/B1. The column was re-equilibrated with 99:1 A1/B1 for 2.0 min before the next run. Each sample was injected two times for analysis in both positive and negative modes. For initial full scan MS (range 300 to 200 *m/z*) the resolution was set to 120,000 with a data dependent MS^2 triggered for any analyte reaching 3e6 or above signal. Data-dependent MS^2 were collected at 30,000 resolution. Lipid species that were different between samples with statistical significance (adjusted p-value <0.05) were identified by the ThermoFisher LipidSearch software package.

2.6. Immunoblotting

Heart tissue from a single animal was homogenized in RIPA buffer with protease and phosphatase inhibitors (Thermo Fisher Scientific, 78446) until visibly homogenized. Homogenates were vortexed well and centrifuged at 10,000*g* for 10 min at 4 °C. The resulting supernatant was transferred to a new tube. Protein content was quantified using a Lowry assay. Ten micrograms of protein were loaded per lane of an Any kD SDS-PAGE gel (Bio-Rad Criterion TGX stain-free precast gels) and transferred to PVDF membranes using Trans-Blot® Turbo™ Transfer System (BIO RAD, 1704150). The membranes were blocked for 1 h. in 5 % BSA. Proteins were detected using HRP-linked anti-mouse secondary antibody (Cell Signaling Technology, 7076, 1:10,000), Clarity ECL Western blotting substrate (Bio-Rad, 1705061) for HRP, and a Chem-iDoc imaging system (BIO RAD, 17001401, 17001402). Blots were assessed for protein expression of CerS2 (Abnova H00029956-M01A, 1:1000, overnight at 4 °C), and stain-free total protein were used to determine even loading. The intensity was quantified using ImageJ.

2.7. Quantitative PCR

Total RNA was isolated from heart tissue of a single animal and homogenized in Trizol (Invitrogen, 15596026) followed by RNeasy mini kit (Qiagen, 74106) extraction and column purification. RNA concentration in tissue was measured using the Agilent 2100 bioanalyzer. cDNA was synthesized from 1 μg of total RNA using iScript Advanced cDNA synthesis kit (Bio-Rad, 1708890). Real-time PCR was performed using a CFX96

Real-Time system (Bio-Rad) and SSoAdvanced Sybr (Bio-Rad, 1725272). The following primers were used: Glyceraldehyde 3-phosphate dehydrogenase (GAPDH) using Qiagen QuantiTect Primers QT01658692; Hydroxymethylbilane Synthetase (Hmbs1; IDT), Fwd 5′ ATGAGGGTGATTCGAGTGGG 3′, Rev 5′ TTGTCTCCCGTGGTGGACATA 3′; and Ceramide Synthase 2 (CerS2; IDT), Fwd 5′ ATGCTCCAGACCTTGTATGACT 3′, Rev 5′ CTGAGGCTTTGG CATAGACAC 3′. Mean normalized expression was calculated by normalizing to the geometric mean of reference genes GAPDH and Hmbs in heart tissue [i.e., $root_2(C_q$ gene 1 × C_q gene 2)] using the $^{\Delta\Delta}C_t$ method, where C_q is the quantitation cycle and C_t is the cycle threshold.

2.8. Statistical analysis

Data are expressed as the mean ± standard deviation [33]. Differences between groups were compared by one-way ANOVA after the data passed normality and equal distribution tests. When a significant F value was obtained, means were compared using the Student-Newman-Keuls test of multiple comparisons. Statistical significance was defined as a value of $p < 0.05$.

3. Results

3.1. Aging altered cardiolipin in the ER

The successful separation of mitochondria, MAM, and ER is shown in Fig. 1A. The inositol tris-phosphate receptor (IP3R) was found in MAM and ER [34]. FACL4 content in MAM was much greater than that in mitochondria and ER, consistent with previously described localization to MAM [2,35]. Cytochrome *c* was located in mitochondria as expected [36]. VDAC was mainly detected in mitochondria, whereas some VDAC was also detected in the MAM and ER. VDAC is expected to be present in MAM [34]. SERCA2 was enriched in ER and not detected in the mitochondria or MAM as previously described [37]. Together these data indicate a robust separation of these cell components.

Compared to 3 mo., total cardiolipin content was dramatically increased in the ER from 18 mo. mice (Fig. 1B). The content of total cardiolipin in 24 mo. ER was still higher than that in 3 mo. mice. However, cardiolipin content was lower in 24 mo. ER compared to 18 mo. (Fig. 1B). There was no significant difference in total cardiolipin content in both MAM (Fig. 1C) and SSM (Fig. 1D) between 3, 18, and 24 mo. mice.

There was some specificity in the chain-length increases in cardiolipins, with a large increase of $(C18:2)_3(C18:3)_1$ and $(C18:2)_2(C18:1)_2$, with less notable differences in the $(C18:2)_4$, $(C18:2)_3(C18:1)_1$, $(C18:2)_3(C18:0)_1$, and $(C18:2)_3(C22:6)_1$ species at 18 months. These increases were attenuated at 24 months but remained elevated relative to young 3 mo. mice. (Fig. 2A). The chain-length composition of cardiolipin was not altered in MAM from 3, 18, and 24 mo. mice (Fig. 2B). The chain-length composition of cardiolipin including [$(C18:2)_2(C18:1)_2$, $(C18:2)_3(C18:0)_1$, $(C18:2)_3(C22:6)_1$, $(C18:2)_2(C18:1)_1(C22:6)_1$, and $(18:2)_2(C22:6)_2$] was slightly decreased in 24 mo. SSM compared to 3 mo. SSM (Fig. 2C).

3.2. Aging increased ceramides in ER and MAM

Relative to modest changes in cardiolipins from 3 to 18 mo. mice, changes in ceramides were more dramatic and for some species, attenuation from 18 to 24 mo. was generally of a smaller magnitude than cardiolipins. Compared to 3 mo., the contents of ceramides including C16:0, C18:0, C20:0, C22:0, C24:1, C24:0, C26:1, and C26:0 were dramatically increased in the ER from 18 mo. mice (Fig. 3A). The contents of ceramides including (C20:0, C22:0, C24:0, C26:1, and C26:0) remained elevated in 24 mo. ER compared to 3 mo. (Fig. 3A), though contents were decreased at 24 mo. of age compared to 18 mo. (Fig. 3A). The content of very long chain ceramide (C26:0) was increased in 18 mo. MAM compared to 3 mo. (Fig. 3B). The contents of ceramides (C24:0 and C26:0) were increased in 24 mo. MAM compared to 3 mo. (Fig. 3B). There were no differences in ceramide content between 3, 18, and 24 mo. SSM (Fig. 3C).

3.3. Aging increased monohexosylceramides in ER

Compared to 3 mo., the contents of monohexosylceramides including (C16:0, C18:1, C18:0, C20:0, C22:0, C24:1, C24:0, C26:1, and C26:0) were increased in the ER from 18 mo. mice (Fig. 4A). The contents of monohexosylceramides including (C16:0, C18:1, C18:0, C22:0, C24:1, C24:0, C26:1, and C26:0) were also increased in 24 mo. ER compared to 3 mo. mice (Fig. 4A), though contents modestly decreased from 18 mo. to 24 mo. of age. There were no differences in contents of monohexosylceramides in MAM (Fig. 4B) and SSM (Fig. 4C) from 3, 18, and 24 mo. mice.

3.4. Aging increased sphingomyelin in ER

Compared to 3 mo., the contents of sphingomyelin including (C14:0, C16:0, C18:1, C18:0, C20:0, C22:0, C24:1, C24:0, C26:1, and C26:0) were increased in the ER from 18 mo. mice (Fig. 5A). The contents of sphingomyelin including (C16:0, C18:0, C20:0, C22:0, C24:1, C24:0, C26:1, and C26:0) were also increased in 24 mo. ER compared to 3 mo. mice (Fig. 5A), although decreases in content from 18 mo. to 24 mo. were evident. There were no differences in contents of sphingomyelin in MAM from 3, 18, and 24 mo. mice (Fig. 4B). The contents of sphingomyelin including (C18:1, C18:0, and C20:0) were increased in 24 mo. SSM compared to 3 mo. SSM (Fig. 5C).

3.5. Aging increases CerS2 content

Lipidomic analyses revealed that age increased very long-chain ceramides (C20:0 and greater) in ER at 24 mo. compared to 3 mo. (Fig. 3A). While the ceramide synthase 2 and 4 isoforms could theoretically generate these chain lengths, CerS4 expression has not been reported in heart, whereas CerS2 has been reported [38,39]. Furthermore, C24:1 ceramide is a unique product of CerS2 [38], and therefore, these data suggested that CerS2 content may increase with age. Immunoblotting for CerS2 demonstrated a dramatic increase in 24 mo. mice compared to 3 mo., supporting that age-induced very long chain ceramides likely increased via increased CerS2 (Fig. 6A). Interestingly, mRNA of CerS2 did not demonstrate an increase in aged mice (Fig. 6B), suggesting the increase in CerS2 may involve protein stability rather than regulation at the level of mRNA.

4. Discussion

Our previous study found that aging led to increased ER stress that contributed to mitochondrial dysfunction by impairing the ETC [8,9]. In the current study, we found that aging increased the cardiolipin content in ER but not in the MAM or SSM (Fig. 1). Aging also increased the contents of ceramide species in both ER and MAM. Interestingly, the contents of sphingomyelin and monohexosylceramides were mainly increased in the 18 mo. ER. Mitochondrial dysfunction occurs in 24 mo. mice [8,9]. These results indicate that alterations of lipid content occur earlier than the onset of mitochondrial dysfunction. The changes in lipid content and composition mainly occur in the ER but not in mitochondria, indicating that alterations in the lipids are likely to alter mitochondrial function as a downstream event during aging. We find that ER stress contributes to mitochondrial dysfunction during aging [8,9]. Alteration of lipids especially ceramide can increase the ER stress [40]. Our results suggest that aging leads to mitochondrial dysfunction by increasing the ER stress potentially through the alteration of ceramide content and composition in the ER.

4.1. Mitochondrial dysfunction and cardiolipin alteration during aging

OXPHOS is decreased in both SSM and IFM from aged C57BL/6 mice [8,9]. Since MAM are separated from the same initial fraction used to subsequently isolate purified SSM [2], only SSM were isolated in the current study. Since cardiolipin is essential to maintain enzyme activity in the ETC [25,41], we first analyzed cardiolipin content and composition in ER, MAM, and mitochondria from the different aged mice.

Our previous studies showed that a decrease in cardiolipin content impairs the ETC in cardiac mitochondria following ischemia [42,43]. Cardiolipin content has been shown to be decreased in a mixed population of cardiac mitochondria in aged rat hearts [29,30]. However, aging does not alter cardiolipin content or composition in SSM or IFM from 24 mo. aged Fischer 344 rats [31]. In agreement with the previous finding in a rat model of aging [31], the current study found that the total cardiolipin content was also not altered in aged mouse heart mitochondria. However, the current study does find that the chain-length compositions of cardiolipin mainly in $(C18:2)_2(C18:1)_2$, $(C18:2)_3(C18:0)_1$, $(C18:2)_3(C22:6)_1$, $(C18:2)_2(C18:1)_1(C22:6)_1$, and $(C18:2)_2(C22:6)_2$ are decreased in 24 mo. mitochondria compared to young mice. Changes in cardiolipin not only affect the activity of individual respiratory complexes, but also impair the formation of respirasomes, so called “supercomplexes” [44]. In supercomplexes, the efficiency of electron transport through the ETC is substantially increased [45,46]. Supercomplexes are decreased in aged heart mitochondria from animals and in human studies [44,46,47]. The mitochondrial targeted drug SS-31 binds to cardiolipin and improves the efficiency of the ETC. SS-31 treatment improves mitochondrial function in aged hearts [48-50], indicating that the cardiolipin defect may indeed contribute to the mitochondrial dysfunction that occurs during aging. Our results suggest that alterations in cardiolipin composition likely contribute to mitochondrial defects during aging.

Cardiolipin is synthesized with interactions between the ER and mitochondria that involve transport into mitochondria through MAM with final remodeling to tetra-linoleoyl

cardiolipin in the mitochondria by the mitochondria-localized enzyme tafazzin [51,52]. Disease altered cardiolipin undergoes remodeling in the MAM and ER, including by the enzyme ALCAT-1 [53]. Since a cardiolipin defect leads to mitochondrial dysfunction, we anticipate that cardiolipin contents are also decreased in the ER and MAM. However, the opposite was found in the aged ER and MAM. Cardiolipin content is increased in the ER from aged mice, potentially indicating enhanced remodeling of cardiolipin that has undergone age-induced oxidative or calcium-mediated damage transferred from mitochondria, the latter by activation of phospholipase A2 to generate monolysocardiolipin [36,54]. Monolysocardiolipin is then remodeled by reacylation in the ER and MAM by ALCAT-1 to cardiolipin which contains non-linoleoyl acyl-groups [36]. The potential of oxidative damage to cardiolipin may occur in response to ER stress, via calcium activated or extrinsic oxidative damage, or in response to age induced defects in the ETC [8]. The lipidomic data suggest the potential for a mutually reinforcing feedback loop between ER and mitochondria to enhance damage and dysfunction in both organelles.

4.2. Mitochondrial dysfunction and ceramide alteration during aging

Aging leads to increased ceramide content and impaired mitochondrial function in aged heart mitochondria [55]. Reduction of the ceramide level in aged rats with lipoic acid treatment restores mitochondrial function in aged rats [55]. An elevation of ceramide content by activating CerS6 decreases OXPHOS during oxidative stress by impairing cytochrome oxidase activity [56]. These studies suggest that changes in ceramide content could directly alter mitochondrial function during aging. In the current study, we find that the content of ceramides is increased in the ER but not in mitochondria from the aged mouse heart (Fig. 3). This result suggests that aging-mediated mitochondrial ceramide alteration does not directly account for the age-induced defects in ETC function in the mouse heart. Although aging increases cytochrome oxidase defects and ROS generation from mouse heart mitochondria [8], the unchanged ceramide contents support that ceramides are not directly the source of the mitochondrial dysfunction in aged mice. In addition to direct inhibition of mitochondrial function, ceramide can indirectly impair mitochondrial function by increasing inflammation and impairing mitophagy. Aging leads to decreased mitophagy and increased ceramide level in mouse skeletal and heart tissue [57]. Changes in ceramides may impair mitochondrial function indirectly in aged mice by decreasing mitophagy thereby allowing the persistence of age-damaged mitochondria [58].

4.3. Ceramide alteration and ER stress during aging

Perturbation of the membrane composition of the ER alters the protein folding environment and thereby can induce ER stress [20]. Ceramide plays a key role in regulating membrane thickness and rigidity. Changes in ceramides can induce ER stress by increasing protein misfolding and aggregation [59]. Ceramide treatment increases Bip expression in rat vascular rings [40]. Ceramide also acts directly through ER stress effectors; IRE1 directly responds to perturbations in its membrane lipid environment, and dihydroceramides directly activate ATF6 [15]. These results support the idea that ceramides are potential inducers of the ER stress. The current study found that the content of several ceramides is increased in ER from hearts during the course of cardiac aging, suggesting that changes in the ceramides is a potential factor to increase the ER stress during aging. Interestingly, the onset of ER

stress in the heart precedes the onset of age-induced mitochondrial defects, suggesting that increased ceramide content present in the ER during aging may induce ER stress and the resulting downstream mitochondrial defects present in the aging murine heart.

4.4. Source of increased ceramide during aging

Ceramides are produced from palmitate and serine to generate the amino alcohol sphinganine that is a substrate for ceramide biosynthesis [16]. Ceramides are synthesized by CerS which are localized in the ER. CerS acylate the nitrogen in sphinganine to generate dihydroceramide. Dihydroceramide is subsequently desaturated to ceramide [16] (Fig. 7). Ceramides can also be generated catabolically by hydrolysis of sphingomyelin or monohexosylceramides [11,16] (Fig. 7). The current study found that aging increased the formation of sphingomyelin and monohexosylceramides, consistent with a previous finding [11]. Aging also leads to increased monohexosylceramides in humans [60]. Caloric restriction prevents the accumulation of long-chain glycosphingolipids and monohexosylceramides during aging [60]. Aging increases the activity of sphingomyelinase that can increase the formation of ceramides from sphingomyelin by catabolism of sphingomyelin [55]. These results support that sphingomyelin and monohexosylceramides are potential sources to increase the ceramide content during aging [60].

There are six isoforms of CerS enzymes that are essential to form ceramides [17,18]. Ceramides are classified according to length of the N-linked fatty acid residue chain length [17,18]. Specific CerS and ceramide molecular species promote distinct biological outcomes. For example, CerS5 utilizes myristoyl- (C14:0) or palmitoyl-CoA (C16:0), yielding medium- (C14) or long-chain (C16:0) ceramides which caused cardiomyocyte hypertrophy [17]. CerS2 generates very long chain ceramides that can increase mitochondrial damage [18]. Inhibition of CerS in *C. elegans* increases autophagy-dependent lifespan extension [61], indicating that CerS-mediated formation of ceramides contributes to the aging process. However, data regarding potential alterations in CerS in aged hearts are limited. The full characterization of the CerS profile in aged hearts to correspond to the profile of molecular species observed during aging in the heart observed in the current study warrants future evaluation.

4.5. Alteration of MAM function during aging

The interaction of the ER with mitochondria occurs through the MAM [62]. The MAM contribute a key role in lipid transfer and calcium exchange from the ER to mitochondria [12,63]. MAM also contribute to the formation of autophagosome formation [62]. A recent study described the distribution of sphingolipids in the MAM [12]. Staurosporine treatment increased apoptosis and the formation of ceramide in the MAM [12]. The activity of sphingomyelinase was increased in the MAM during staurosporine treatment [12]. These results indicate that staurosporine-induced sphingomyelinase activity augments ceramide formation. The current study found that aging increased the content of ceramides, especially long-chain ceramides, in the MAM (Fig. 3). The activity of sphingomyelinase is increased during aging [55]. The increased ceramide content in MAM in the current study may be due to activation of sphingomyelinase. The mechanism of generation of the increased ceramide content in the MAM with aging requires future study.

Disruption of MAM function by inducing changes in sphingolipids increases apoptosis [12] and decreases autophagosome formation [62]. The MAM dysfunction can impair calcium transfer between mitochondria and ER [63]. Calcium overload is known to induce mitochondrial dysfunction [25]. An increase in calcium can sensitize to mitochondrial permeability transition pore opening [64,65]. Calcium overload can damage the ETC by activating calcium-dependent proteases including calpains [66,67]. Thus, alteration of sphingolipids in the MAM can contribute to mitochondrial dysfunction during aging by impairing autophagy and calcium balance.

4.6. Conclusion

Aging leads to cardiac mitochondrial dysfunction by increasing the ER stress [8,9]. The findings in the current study support that age-induced alteration of sphingolipids likely contributes to the increased ER stress. Restoration of sphingolipid balance is a potential strategy to improve mitochondrial function in aged hearts.

Acknowledgements

This work was supported by the Office of Research and Development, Medical Research Service Merit Review Award (2IO1BX001355-01A2) (QC, EJL) and I01BX002000 (LAC), the National Institute of Aging (NIA) R21AG054975-01 and a Pauley Pilot Grant (QC), the National Heart Lung & Blood Institute R01HL151243 (LAC), and the Pauley Heart Center, Virginia Commonwealth University (QC, JT, YH, EJL). Services in support of the research project were provided by the VCU Massey Cancer Center Lipidomics and Metabolomics Shared Resource, supported, in part, with funding from NIH-NCI Cancer Center Support Grant P30 CA016059.

Data availability

Data will be made available on request.

References

[1]. Veerasamy M, Ford GA, Neely D, Bagnall A, MacGowan G, Das R, Kunadian V, Association of aging, arterial stiffness, and cardiovascular disease: a review, Cardiol. Rev 22 (2014) 223–232. [PubMed: 24441048]

[2]. Wieckowski MR, Giorgi C, Lebiedzinska M, Duszynski J, Pinton P, Isolation of mitochondria-associated membranes and mitochondria from animal tissues and cells, Nat. Protoc 4 (2009) 1582–1590. [PubMed: 19816421]

[3]. Zhou H, Wang S, Hu S, Chen Y, Ren J, ER-mitochondria microdomains in cardiac ischemia-reperfusion injury: a fresh perspective, Front. Physiol 9 (2018) 755. [PubMed: 29962971]

[4]. Sciarretta S, Zhai P, Shao D, Zablocki D, Nagarajan N, Terada LS, Volpe M, Sadoshima J, Activation of NADPH oxidase 4 in the endoplasmic reticulum promotes cardiomyocyte autophagy and survival during energy stress through the protein kinase RNA-activated-like endoplasmic reticulum kinase/eukaryotic initiation factor 2alpha/activating transcription factor 4 pathway, Circ. Res 113 (2013) 1253–1264. [PubMed: 24081881]

[5]. Zhang Y, Ren J, Thapsigargin triggers cardiac contractile dysfunction via NADPH oxidase-mediated mitochondrial dysfunction: role of Akt dephosphorylation, Free Radic. Biol. Med 51 (2011) 2172–2184. [PubMed: 21996563]

[6]. Chen Q, Thompson J, Hu Y, Das A, Lesnefsky EJ, Metformin attenuates ER stress-induced mitochondrial dysfunction, Transl. Res 190 (2017) 40–50. [PubMed: 29040818]

[7]. Chen Q, Thompson J, Hu Y, Das A, Lesnefsky EJ, Cardiac specific knockout of p53 decreases ER stress-induced mitochondrial damage, Front. Cardiovasc. Med 6 (2019) 10. [PubMed: 30838215]

[8]. Chen Q, Samidurai A, Thompson J, Hu Y, Das A, Willard B, Lesnefsky EJ, Endoplasmic reticulum stress-mediated mitochondrial dysfunction in aged hearts, Biochim. Biophys. Acta Mol. basis Dis 1866 (2020), 165899. [PubMed: 32698045]

[9]. Chen Q, Thompson J, Hu Y, Lesnefsky EJ, Chronic metformin treatment decreases cardiac injury during ischemia-reperfusion by attenuating endoplasmic reticulum stress with improved mitochondrial function, Aging (Albany NY) 13 (2021) 7828–7845. [PubMed: 33746115]

[10]. Strub GM, Paillard M, Liang J, Gomez L, Allegood JC, Hait NC, Maceyka M, Price MM, Chen Q, Simpson DC, Kordula T, Milstien S, Lesnefsky EJ, Spiegel S, Sphingosine-1-phosphate produced by sphingosine kinase 2 in mitochondria interacts with prohibitin 2 to regulate complex IV assembly and respiration, FASEB J. 25 (2011) 600–612. [PubMed: 20959514]

[11]. Vozella V, Basit A, Misto A, Piomelli D, Age-dependent changes in nervonic acid-containing sphingolipids in mouse hippocampus, Biochim. Biophys. Acta Mol. Cell Biol. Lipids 2017 (1862) 1502–1511.

[12]. Mignard V, Dubois N, Lanoé D, Joalland MP, Oliver L, Pecqueur C, Heymann D, Paris F, Vallette FM, Lalier L, Sphingolipid distribution at mitochondria-associated membranes (MAMs) upon induction of apoptosis, J. Lipid Res 61 (2020) 1025–1037. [PubMed: 32350079]

[13]. Gomez L, Paillard M, Price M, Chen Q, Teixeira G, Spiegel S, Lesnefsky EJ, A novel role for mitochondrial sphingosine-1-phosphate produced by sphingosine kinase-2 in PTP-mediated cell survival during cardioprotection, Basic Res. Cardiol 106 (2011) 1341–1353. [PubMed: 22002221]

[14]. Chipuk JE, McStay GP, Bharti A, Kuwana T, Clarke CJ, Siskind LJ, Obeid LM, Green DR, Sphingolipid metabolism cooperates with BAK and BAX to promote the mitochondrial pathway of apoptosis, Cell 148 (2012) 988–1000. [PubMed: 22385963]

[15]. Tam AB, Roberts LS, Chandra V, Rivera IG, Nomura DK, Forbes DJ, Niwa M, The UPR activator ATF6 responds to proteotoxic and lipotoxic stress by distinct mechanisms, Dev. Cell 46 (2018) 327–343.e327. [PubMed: 30086303]

[16]. Walls SM, Cammarato A, Chatfield DA, Ocorr K, Harris GL, Bodmer R, Ceramide-protein interactions modulate ceramide-associated lipotoxic cardiomyopathy, Cell Rep. 22 (2018) 2702–2715. [PubMed: 29514098]

[17]. Russo SB, Baicu CF, Van Laer A, Geng T, Kasiganesan H, Zile MR, Cowart LA, Ceramide synthase 5 mediates lipid-induced autophagy and hypertrophy in cardiomyocytes, J. Clin. Invest 122 (2012) 3919–3930. [PubMed: 23023704]

[18]. Law BA, Liao X, Moore KS, Southard A, Roddy P, Ji R, Szulc Z, Bielawska A, Schulze PC, Cowart LA, Lipotoxic very-long-chain ceramides cause mitochondrial dysfunction, oxidative stress, and cell death in cardiomyocytes, FASEB J. 32 (2018) 1403–1416. [PubMed: 29127192]

[19]. Guan C, Zhang HF, Wang YJ, Chen ZT, Deng BQ, Qiu Q, Chen SX, Wu MX, Chen YX, Wang JF, The downregulation of ADAM17 exerts protective effects against cardiac fibrosis by regulating endoplasmic reticulum stress and mitophagy, Oxidative Med. Cell. Longev 2021 (2021) 5572088.

[20]. Ho N, Xu C, Thibault G, From the unfolded protein response to metabolic diseases - lipids under the spotlight, J. Cell Sci 131 (2018).

[21]. Liu Z, Xia Y, Li B, Xu H, Wang C, Liu Y, Li Y, Li C, Gao N, Li L, Induction of ER stress-mediated apoptosis by ceramide via disruption of ER Ca(2+) homeostasis in human adenoid cystic carcinoma cells, Cell Biosci. 4 (2014) 71. [PubMed: 25937892]

[22]. Sundaram K, Mather AR, Marimuthu S, Shah PP, Snider AJ, Obeid LM, Hannun YA, Beverly LJ, Siskind LJ, Loss of neutral ceramidase protects cells from nutrient- and energy -deprivation-induced cell death, Biochem. J 473 (2016) 743–755. [PubMed: 26747710]

[23]. Bennett MK, Wallington-Beddoe CT, Pitson SM, Sphingolipids and the unfolded protein response, Biochim. Biophys. Acta Mol. Cell Biol. Lipids 2019 (1864) 1483–1494.

[24]. Montgomery MK, Brown SH, Lim XY, Fiveash CE, Osborne B, Bentley NL, Braude JP, Mitchell TW, Coster AC, Don AS, Cooney GJ, Schmitz-Peiffer C, Turner N, Regulation of glucose homeostasis and insulin action by ceramide acyl-chain length: a beneficial role for very long-chain sphingolipid species, Biochim. Biophys. Acta 2016 (1861) 1828–1839.

[25]. Lesnefsky EJ, Chen Q, Hoppel CL, Mitochondrial metabolism in aging heart, Circ. Res 118 (2016) 1593–1611. [PubMed: 27174952]

[26]. Hoch FL, Cardiolipins and biomembrane function, Biochim. Biophys. Acta 1113 (1992) 71–133. [PubMed: 1550861]

[27]. Houtkooper RH, Vaz FM, Cardiolipin, the heart of mitochondrial metabolism, Cell. Mol. Life Sci 65 (2008) 2493–2506. [PubMed: 18425414]

[28]. Lesnefsky EJ, Hoppel CL, Cardiolipin as an oxidative target in cardiac mitochondria in the aged rat, Biochim. Biophys. Acta 1777 (2008) 1020–1027. [PubMed: 18515061]

[29]. Paradies G, Ruggiero FM, Dinoi P, Petrosillo G, Quagliariello E, Age-dependent decrease in the cytochrome c oxidase activity and changes in phopsholiids in rat-heart mitochondria, Arch. Gerontol. Geriatr 16 (1993) 262–272.

[30]. Paradies G, Ruggiero FM, Petrosillo G, Quagliariello E, Age-dependent decline in the cytochrome c oxidase activity in rat heart mitochondria: role of cardiolipin, FEBS Lett. 406 (1997) 136–138. [PubMed: 9109403]

[31]. Moghaddas S, Stoll MS, Minkler PE, Salomon RG, Hoppel CL, Lesnefsky EJ, Preservation of cardiolipin content during aging in rat heart interfibrillar mitochondria, J. Gerontol. A Biol. Sci. Med. Sci 57 (2002) B22–B28. [PubMed: 11773203]

[32]. Van Veldhoven PP, Bell RM, Effect of harvesting methods, growth conditions and growth phase on diacylglycerol levels in cultured human adherent cells, Biochim. Biophys. Acta 959 (1988) 185–196. [PubMed: 3349097]

[33]. Steel R, Torrie J, Principles and Procedures of Statistics, Mc Graw-Hill, New York, 1960.

[34]. Duponchel S, Monnier L, Molle J, Bendridi N, Alam MR, Gaballah A, Grigorov A, Ivanov A, Schmiel M, Odenthal M, Ovize M, Rieusset J, Zoulim F, Bartosch B, Hepatitis C virus replication requires integrity of mitochondria-associated ER membranes, JHEP Rep. 5 (2023), 100647. [PubMed: 36718430]

[35]. Horner SM, Wilkins C, Badil S, Iskarpatyoti J, Gale M Jr., Proteomic analysis of mitochondrial-associated ER membranes (MAM) during RNA virus infection reveals dynamic changes in protein and organelle trafficking, PLoS One 10 (2015), e0117963. [PubMed: 25734423]

[36]. Cao J, Liu Y, Lockwood J, Burn P, Shi Y, A novel cardiolipin-remodeling pathway revealed by a gene encoding an endoplasmic reticulum-associated acyl-CoA:lysocardiolipin acyltransferase (ALCAT1) in mouse, J. Biol. Chem 279 (2004) 31727–31734. [PubMed: 15152008]

[37]. Paillard M, Tubbs E, Thiebaut PA, Gomez L, Fauconnier J, Da Silva CC, Teixeira G, Mewton N, Belaidi E, Durand A, Abrial M, Lacampagne A, Rieusset J, Ovize M, Depressing mitochondria-reticulum interactions protects cardiomyocytes from lethal hypoxia-reoxygenation injury, Circulation 128 (2013) 1555–1565. [PubMed: 23983249]

[38]. Zhang X, Sakamoto W, Canals D, Ishibashi M, Matsuda M, Nishida K, Toyoshima M, Shigeta S, Taniguchi M, Senkal CE, Okazaki T, Yaegashi N, Hannun YA, Nabe T, Kitatani K, Ceramide synthase 2-C(24:1)-ceramide axis limits the metastatic potential of ovarian cancer cells, FASEB J. 35 (2021), e21287. [PubMed: 33423335]

[39]. Kretzschmar T, Bekhite MM, Wu JMF, Haase D, Förster M, Müller T, Nietzsche S, Westermann M, Franz M, Gräler MH, Schulze PC, Long-chain and very long-chain ceramides mediate doxorubicin-induced toxicity and fibrosis, Int. J. Mol. Sci 22 (2021).

[40]. Zhang H, Li J, Li L, Liu P, Wei Y, Qian Z, Ceramide enhances COX-2 expression and VSMC contractile hyperreactivity via ER stress signal activation, Vasc. Pharmacol 96-98 (2017) 26–32.

[41]. Lesnefsky EJ, Hoppel CL, Oxidative phosphorylation and aging, Ageing Res. Rev 5 (2006) 402–433. [PubMed: 16831573]

[42]. Lesnefsky EJ, Chen Q, Moghaddas S, Hassan MO, Tandler B, Hoppel CL, Blockade of electron transport during ischemia protects cardiac mitochondria, J. Biol. Chem 279 (2004) 47961–47967. [PubMed: 15347666]

[43]. Lesnefsky EJ, Slabe TJ, Stoll MS, Minkler PE, Hoppel CL, Myocardial ischemia selectively depletes cardiolipin in rabbit heart subsarcolemmal mitochondria, Am. J. Phys 280 (2001) H2770–H2778.

[44]. Gomez LA, Monette JS, Chavez JD, Maier CS, Hagen TM, Supercomplexes of the mitochondrial electron transport chain decline in the aging rat heart, Arch. Biochem. Biophys 490 (2009) 30–35. [PubMed: 19679098]

[45]. Rosea M, Minkler P, Hoppel CL, Cardiac mitochondria in heart failure: normal cardiolipin profile and increased threonine phosphorylation of complex IV, Biochim. Biophys. Acta 2011 (1807) 1373–1382.

[46]. Genova ML, Lenaz G, The interplay between respiratory supercomplexes and ROS in aging, Antioxid. Redox Signal 23 (2015) 208–238. [PubMed: 25711676]

[47]. Sgarbi G, Matarrese P, Pinti M, Lanzarini C, Ascione B, Gibellini L, Dika E, Patrizi A, Tommasino C, Capri M, Cossarizza A, Baracca A, Lenaz G, Solaini G, Franceschi A, Malorni W, Salvioli S, Mitochondria hyperfusion and elevated autophagic activity are key mechanisms for cellular bioenergetic preservation in centenarians, Aging (Albany NY) 6 (2014) 296–310. [PubMed: 24799450]

[48]. Whitson JA, Bitto A, Zhang H, Sweetwyne MT, Coig R, Bhayana S, Shankland EG, Wang L, Bammler TK, Mills KF, Imai SI, Conley KE, Marcinek DJ, Rabinovitch PS, SS-31 and NMN: two paths to improve metabolism and function in aged hearts, Aging Cell 19 (2020), e13213. [PubMed: 32779818]

[49]. Zhang H, Alder NN, Wang W, Szeto H, Marcinek DJ, Rabinovitch PS, Reduction of elevated proton leak rejuvenates mitochondria in the aged cardiomyocyte, Elife 9 (2020).

[50]. Whitson JA, Martín-Pérez M, Zhang T, Gaffrey MJ, Merrihew GE, Huang E, White CC, Kavanagh TJ, Qian WJ, Campbell MD, MacCoss MJ, Marcinek DJ, Villén J, Rabinovitch PS, Elamipretide (SS-31) treatment attenuates age-associated post-translational modifications of heart proteins, Geroscience 43 (2021) 2395–2412. [PubMed: 34480713]

[51]. Sparagna GC, Johnson CA, McCune SA, Moore RL, Murphy RC, Quantitation of cardiolipin molecular species in spontaneously hypertensive heart failure rats using electrospray ionization mass spectrometry, J. Lipid Res 46 (2005) 1196–1204. [PubMed: 15772420]

[52]. Sparagna GC, Lesnefsky EJ, Cardiolipin remodeling in the heart, J. Cardiovasc. Pharmacol 53 (2009) 290–301. [PubMed: 19276988]

[53]. Jia D, Zhang J, Nie J, Andersen JP, Rendon S, Zheng Y, Liu X, Tian Z, Shi Y, Cardiolipin remodeling by ALCAT1 links hypoxia to coronary artery disease by promoting mitochondrial dysfunction, Mol. Ther 29 (2021) 3498–3511. [PubMed: 34111561]

[54]. Seleznev K, Zhao C, Zhang XH, Song K, Ma ZA, Calcium-independent phospholipase A2 localizes in and protects mitochondria during apoptotic induction by staurosporine, J. Biol. Chem 281 (2006) 22275–22288. [PubMed: 16728389]

[55]. Monette JS, Gómez LA, Moreau RF, Dunn KC, Butler JA, Finlay LA, Michels AJ, Shay KP, Smith EJ, Hagen TM, (R)-α-lipoic acid treatment restores ceramide balance in aging rat cardiac mitochondria, Pharmacol. Res 63 (2011) 23–29. [PubMed: 20934512]

[56]. Schüll S, Günther SD, Brodesser S, Seeger JM, Tosetti B, Wiegmann K, Pongratz C, Diaz F, Witt A, Andree M, Brinkmann K, Krönke M, Wiesner RJ, Kashkar H, Cytochrome c oxidase deficiency accelerates mitochondrial apoptosis by activating ceramide synthase 6, Cell Death Dis. 6 (2015), e1691. [PubMed: 25766330]

[57]. Zhou J, Chong SY, Lim A, Singh BK, Sinha RA, Salmon AB, Yen PM, Changes in macroautophagy, chaperone-mediated autophagy, and mitochondrial metabolism in murine skeletal and cardiac muscle during aging, Aging (Albany NY) 9 (2017) 583–599. [PubMed: 28238968]

[58]. Liang W, Moyzis AG, Lampert MA, Diao RY, Najor RH, Gustafsson ÅB, Aging is associated with a decline in Atg9b-mediated autophagosome formation and appearance of enlarged mitochondria in the heart, Aging Cell 19 (2020), e13187. [PubMed: 32627317]

[59]. Rao RP, Scheffer L, Srideshikan SM, Parthibane V, Kosakowska-Cholody T, Masood MA, Nagashima K, Gudla P, Lockett S, Acharya U, Acharya JK, Ceramide transfer protein deficiency compromises organelle function and leads to senescence in primary cells, PLoS One 9 (2014), e92142. [PubMed: 24642596]

[60]. Hernández-Corbacho MJ, Jenkins RW, Clarke CJ, Hannun YA, Obeid LM, Snider AJ, Siskind LJ, Accumulation of long-chain glycosphingolipids during aging is prevented by caloric restriction, PLoS One 6 (2011), e20411. [PubMed: 21687659]

[61]. Mosbech MB, Kruse R, Harvald EB, Olsen AS, Gallego SF, Hannibal-Bach HK, Ejsing CS, Færgeman NJ, Functional loss of two ceramide synthases elicits autophagy-dependent lifespan extension in C. elegans, PLoS One 8 (2013), e70087. [PubMed: 23894595]

[62]. Garofalo T, Matarrese P, Manganelli V, Marconi M, Tinari A, Gambardella L, Faggioni A, Misasi R, Sorice M, Malorni W, Evidence for the involvement of lipid rafts localized at the ER-mitochondria associated membranes in autophagosome formation, Autophagy 12 (2016) 917–935. [PubMed: 27123544]

[63]. van Vliet AR, Verfaillie T, Agostinis P, New functions of mitochondria associated membranes in cellular signaling, Biochim. Biophys. Acta 2014 (1843) 2253–2262.

[64]. Murphy E, Steenbergen C, Preconditioning: the mitochondrial connection, Annu. Rev. Physiol 69 (2007) 51–67. [PubMed: 17007587]

[65]. Halestrap AP, Clarke SJ, Javadov SA, Mitochondrial permeability transition pore opening during myocardial reperfusion–a target for cardioprotection, Cardiovasc. Res 61 (2004) 372–385. [PubMed: 14962470]

[66]. Chen Q, Thompson J, Hu Y, Dean J, Lesnefsky EJ, Inhibition of the ubiquitous calpains protects complex I activity and enables improved mitophagy in the heart following ischemia-reperfusion, Am. J. Physiol. Cell Physiol 317 (2019) C910–c921. [PubMed: 31411917]

[67]. Thompson J, Maceyka M, Chen Q, Targeting ER stress and calpain activation to reverse age-dependent mitochondrial damage in the heart, Mech. Ageing Dev 192 (2020), 111380. [PubMed: 33045249]

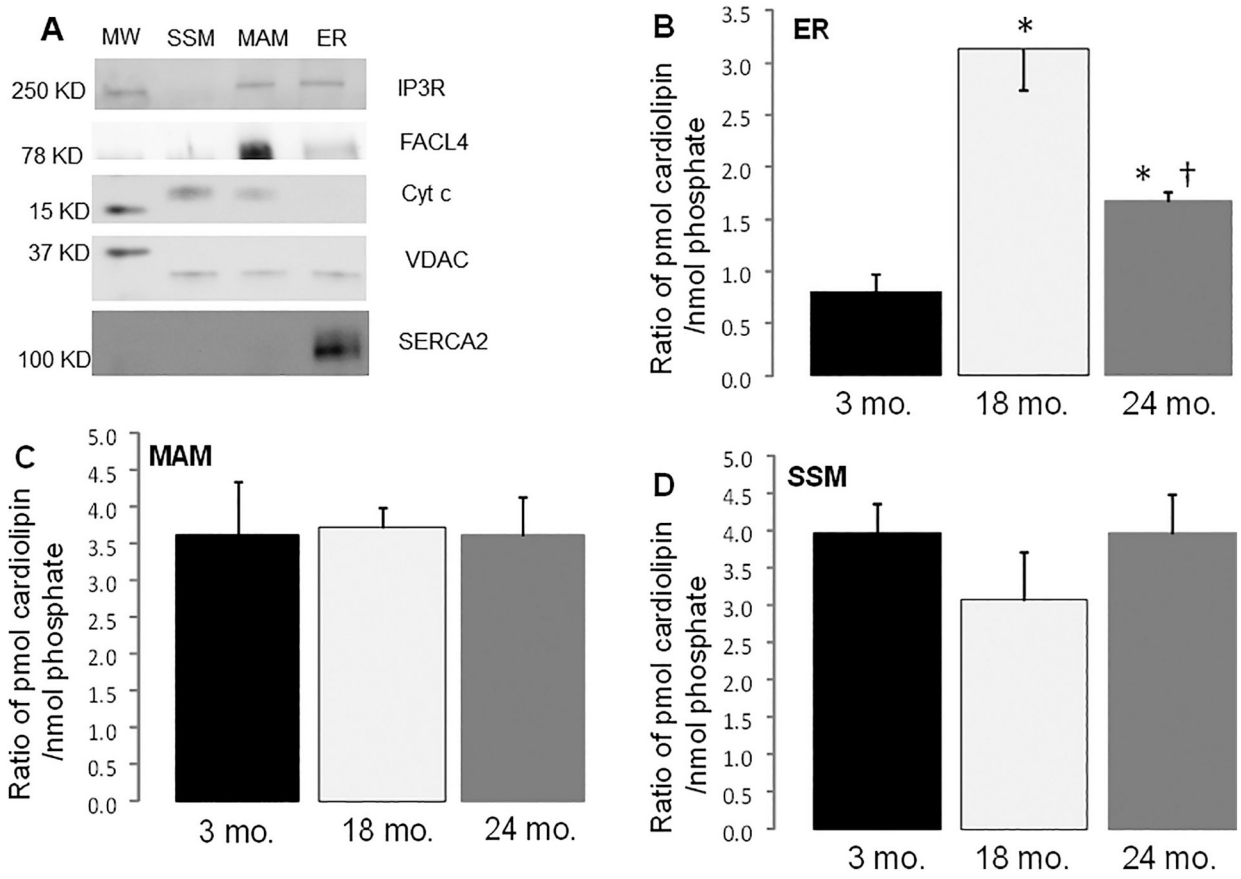

Fig. 1.

Cardiolipin content in ER, MAM, and SSM from different aged hearts.

Panel A shows the separated SSM, MAM, and ER. Cytochrome c (Cyt c) and VDAC were mainly detected in SSM, whereas FACL4 was mainly detected in the MAM. IP3R was found in MAM and ER. SERCA2 was mainly found in the ER. These marker enzyme findings are as expected and support a robust separation of the respective fractions (see text). Panel B shows the elevated content of cardiolipin in ER isolated from 18 mo. and 24 mo. aging hearts compared to 3 mo. adult controls. Cardiolipin content in ER from 24 mo. aged hearts was lower than that in ER from 18 mo. old hearts. There were no significant differences in cardiolipin content in mitochondrial associated membranes (MAM) isolated from 3, 18, and 24 mo. hearts in Panel C nor in subsarcolemmal mitochondria (SSM) isolated from 3, 18, and 24 mo. old hearts shown in Panel D. (Mean ± SEM; *$p < 0.05$ vs. 3 mo. †$p < 0.05$ vs. 18 mo. $n = 5$ in each group).

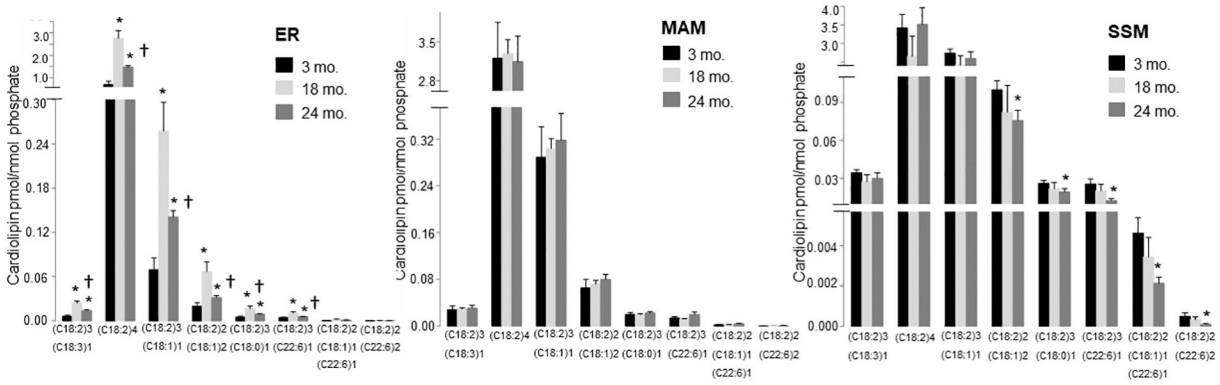

Fig. 2.

Alteration of cardiolipin composition in ER, MAM, and SSM isolated from different aged hearts: Panel A (Left Panel) shows the composition of cardiolipin in ER isolated from 3, 18, and 24 mo. hearts. The contents of several cardiolipin molecular species including $(C18:2)_3(C18:3)_1$, $(C18:2)_4$, $(C18:2)_3(C18:1)_1$, $(C18:2)_2(C18:1)_2$, $(C18:2)_3(C18:0)_1$, and $(C18:2)_3(C22:6)_1$ were elevated in endoplasmic reticulum (ER) isolated from 18 mo. and 24 mo. hearts compared to 3 mo. adult controls. There were no significant differences in the contents of cardiolipin molecular species in mitochondrial associated membranes (MAM) isolated from 3, 18, and 24 mo. hearts as shown in Panel B (Middle Panel). The contents of cardiolipin components were also similar in subsarcolemmal mitochondria (SSM) isolated from 3 and 18 mo. old hearts. However, the contents of several cardiolipin molecular species $(C18:2)_2(C18:1)_2$, $(C18:2)_3(C18:0)_1$, $(C18:2)_3(C22:6)_1$, $(C18:2)_2(C18:1)_1(C22:6)_1$, and $(C18:2)_2(C22:6)_2$ were decreased in SSM isolated from 24 mo. elderly compared to 3 mo. adult hearts as shown in Panel C (Right Panel). Mean ± SEM. *$p < 0.05$ vs. 3 mo. †$p < 0.05$ vs. 18 mo. $n = 5$ in each group.

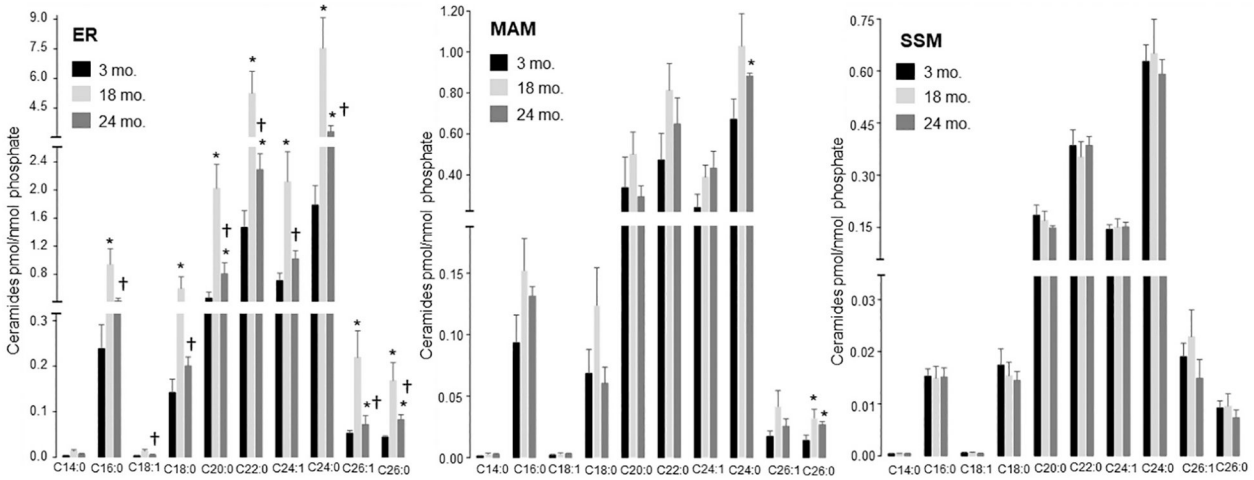

Fig. 3.

Alteration of ceramide composition in ER, MAM, and SSM isolated from different aged hearts.

Panel A (Left Panel) shows the composition of ceramide molecular species in endoplasmic reticulum (ER) isolated from 3, 18, and 24 mo. hearts during the progression of aging. The contents of C16:0, C18:0, C20:0, C22:0, C24:1, C24:0, C26:1, and C26:0 were increased in ER isolated from 18 mo. old hearts compared to 3 mo. adult controls. The contents of ceramide molecular species including C16:0, C20:0, C22:0, C24:0, C26:1, and C26:0 were also increased in ER from 24 mo. aged hearts compared to 3 mo. old adult controls, though decreased from 18 mo. Panel B (Middle Panel) showed that the contents of C24:0 and C26:0 ceramides were increased in mitochondrial associated membranes (MAM) isolated from 24 mo. old aged hearts compared to 3 mo. adult controls. The content of ceramide (C26:0) was also increased in MAM isolated from 18 mo. old hearts vs. 3 mo. adult controls. There were no significant differences in ceramide content in subsarcolemmal mitochondria (SSM) isolated from 3, 18, and 24 mo. old hearts shown in Panel C (Right Panel). Mean ± SEM. *$p < 0.05$ vs. 3 mo. †$p < 0.05$ vs. 18 mo. $n = 5$ in each group.

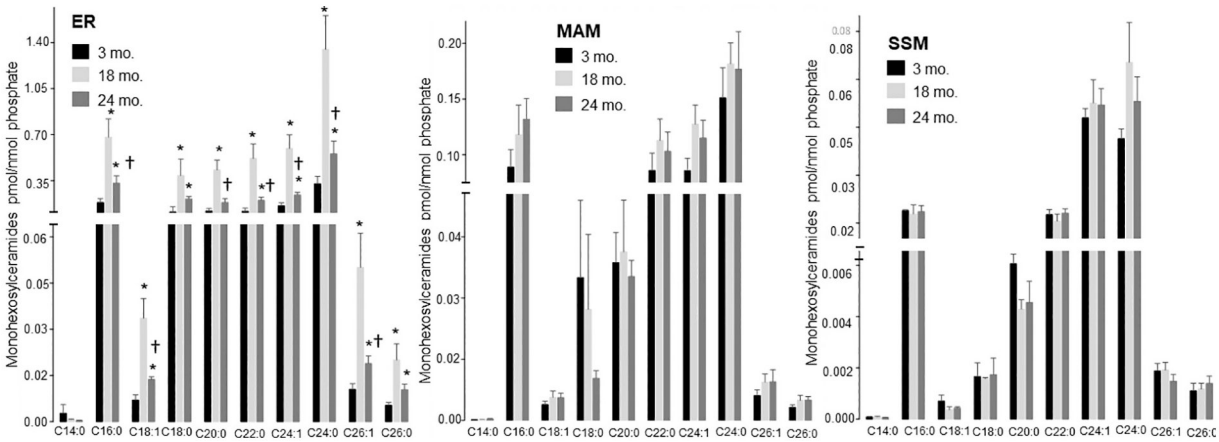

Fig. 4.

Alteration of monohexosylceramides in ER, MAM, and SSM from different aged hearts. Panel A (Left Panel) shows the composition of monohexosylceramide molecular species in endoplasmic reticulum (ER) isolated from 3, 18, and 24 mo. hearts during the progression of aging. The contents of monohexosylceramides including C16:0, C18:1, C18:0, C20:0, C22:0, C24:1, C24:0, C26:1, and C26:0 were increased in ER isolated from 18 mo. and 24 mo. old hearts compared to 3 mo. adult controls. There were no significant differences in the contents of monohexosylceramides in mitochondrial associated membranes (MAM) isolated from in 3, 18, and 24 mo. hearts (Panel B, Middle Panel) nor in subsarcolemmal mitochondria (SSM) (Panel C, Right Panel). Mean ± SEM. *$p < 0.05$ vs. 3 mo. †$p < 0.05$ vs. 18 mo. $n = 5$ in each group.

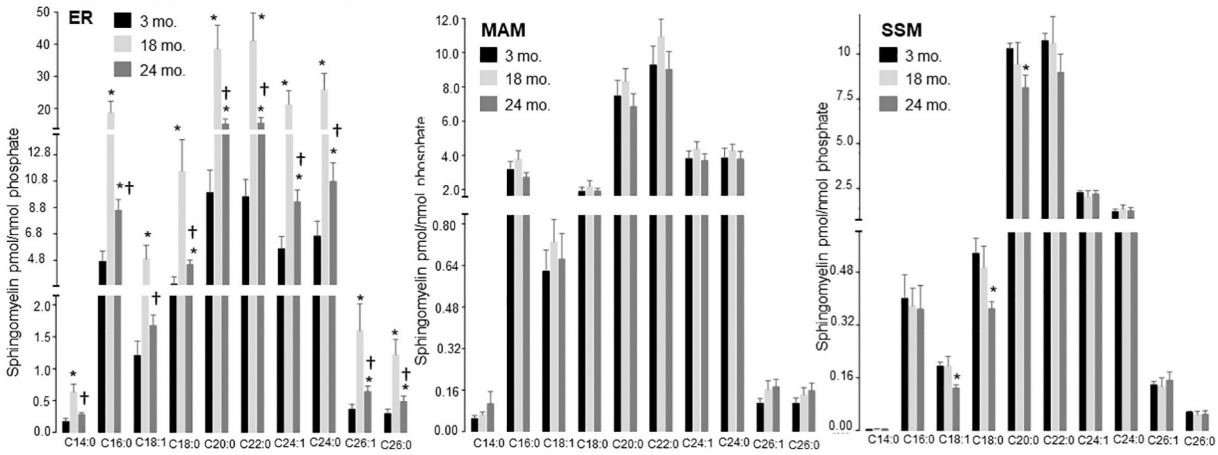

Fig. 5.

Alteration of sphingomyelin in ER, MAM, and SSM from different aged hearts.

Panel A (Left Panel) shows the composition of sphingomyelin molecular species in endoplasmic reticulum (ER) isolated from 3, 18, and 24 mo. hearts. The contents of C14:0, C16:0, C18:1, C18:0, C20:0, C22:0, C24:1, C24:0, C26:1, and C26:0 sphingomyelins were increased in ER isolated from 18 mo. aged hearts compared to 3 mo. adult controls. The contents of sphingomyelins including C16:0, C18:0, C20:0, C22:0, C24:1, C24:0, C26:1, and C26:0 were also increased in ER from 24 mo. elderly hearts compared to 3 mo. old adult controls. There were no significant differences in the contents of sphingomyelin molecular species in mitochondrial associated membranes (MAM) isolated from in 3, 18, and 24 mo. hearts (Panel B, Middle Panel). Panel C (Right Panel) shows that there were no differences in sphingomyelin contents in subsarcolemmal mitochondria (SSM) isolated from 3 mo. and 18 mo. old hearts. However, the content of several sphingomyelin species including C18:1, C18:0, and C20:0 were increased in SSM from 24 mo. elderly compared to 3 mo. adult hearts. Mean ± SEM. *$p < 0.05$ vs. 3 mo. †$p < 0.05$ vs. 18 mo. $n = 5$ in each group.

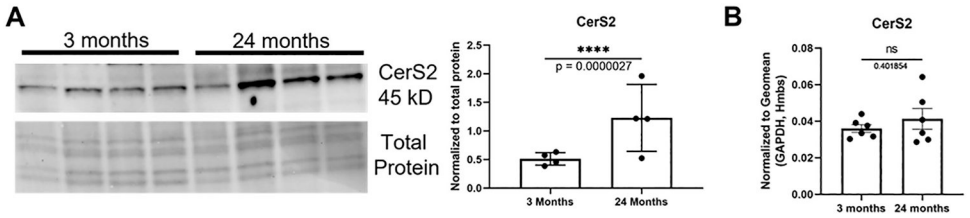

Fig. 6.

Content of ceramide synthase 2 is increased in the aging heart.

Hearts from 24-month aged mice show increased ceramide synthase 2 (CerS2) content relative to 3 mo. adult control mice. Panel A (Left Panel) displays CerS2 protein expression of hearts isolated from 3- and 24- mo. mice. ImageJ was used to quantify the blots, and normalized to total protein (Mean ± SEM. ****$p < 0.01$ vs. 3 mo. n = 4/group). Panel B (Right Panel) shows CerS2 mRNA expression from 3- and 24-month hearts (Mean ± SEM. p = ns between groups. n = 6/group). Each N represents an individual animal.

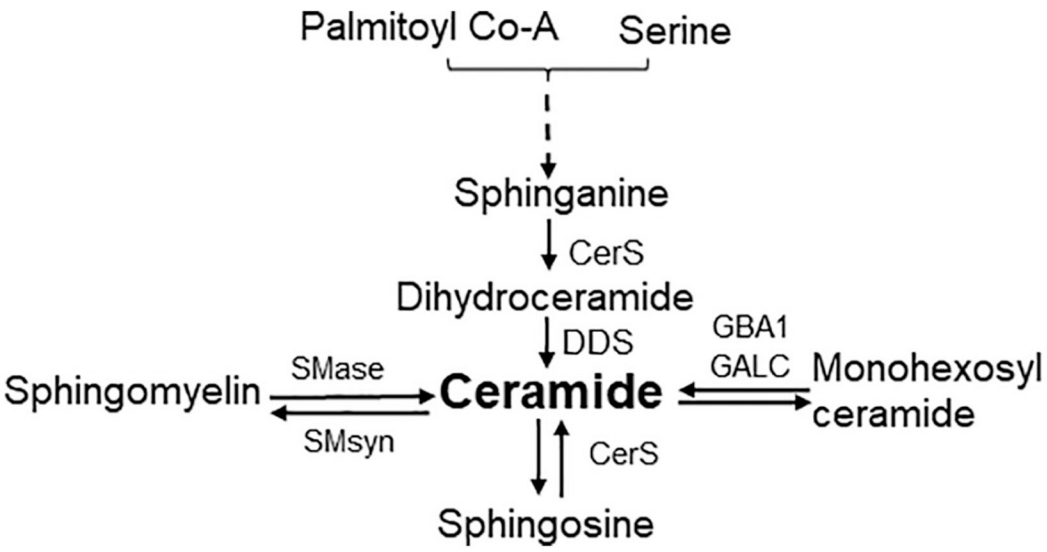

Fig. 7.

Depiction of pathways for ceramide synthesis.

Dihydroceramide is synthesized by ceramide synthase enzymes (CerS) using Palmitoyl Co-A and Serine or sphingosine as substrates. The dihydroceramide is processed by dihydroceramide desaturase (DDS) to generate ceramide. Ceramide can also be generated catabolically through hydrolysis of sphingomyelin by *sphingomyelinase* (SMase). Ceramide is also be generated through hydrolysis of monohexosylceramides in the presence of glucocerebrosidase 1 (GBA1) or galactosylceramidase (GALC). Ceramide can serve as a substrate in the formation of sphingomyelin via sphingomyelin synthase (SMsyn) and sphingosines via the action of ceramidase (Cerase).